Impact of data assimilation on a calibrated WRF model for the prediction of tropical cyclones over the Bay of Bengal

Harish Baki[1], C. Balaji[1,2,3,*] and Balaji Srinivasan[1]

[1]Department of Mechanical Engineering, Indian Institute of Technology Madras, Chennai 600 036, India
[2]Center of Excellence in Atmospheric and Climate Sciences, Indian Institute of Technology Madras, Chennai 600 036, India
[3]Divecha Centre for Climate Change, Indian Institute of Science, Bengaluru 560 012, India

The main objective of the present study is to examine the impact of three-dimensional variational data assimilation utilizing the multivariate background error covariance (BEC) estimates, in combination with the model calibration, for the simulations of seven tropical cyclones over the Bay of Bengal region. The study indicates that the utilization of multivariate BEC in assimilation influences the model forecasts in terms of wind speed at 10 m height, precipitation, cyclone tracks and cyclone intensity. The assimilation experiments conducted with a previously calibrated model combined with the control variable option 6 (cv6) of BEC have reduced the overall root mean square error (RMSE) of 10 m wind speed by 17.02%, precipitation by 11.14%, cyclone track by 41.93% and the intensity by 25.5% when compared to the default model simulations without assimilation. The best experimental setup is then used for the operational forecast of a recent cyclone Gulab. The results show an RMSE reduction of 18.61% in the cyclone track and 28.99% in intensity forecasts. These results also confirm that the utilization of cv6 BEC in the assimilation of conventional and radiance observations on a calibrated model improves the forecast of tropical cyclones over the Bay of Bengal region.

Keywords: Data assimilation, model calibration, multivariate background error statistics, operational forecast, tropical cyclones.

TROPICAL cyclones are one of the most disastrous weather phenomena that affect millions of lives across the globe. The north Indian Ocean contributes to 6–7% of global tropical cyclones[1], with the world's deadliest tropical cyclones often originating from this region. Since the population near coastal regions around the Bay of Bengal (BoB) is increasing, the potential for more damage to lives and property due to tropical cyclones is high[2,3]. In addition, the changing climate and global warming are likely to produce more intense tropical cyclones in the future, which may further result in greater damage to lives and property[4,5]. To mitigate the devastating effects of tropical cyclones, first an accurate prediction of the cyclone track, intensity and precipitation during landfall is required.

The use of numerical weather prediction (NWP) models for the prediction of tropical cyclones gained popularity in the late 1960s (ref. 6). From then, the NWP models have evolved to a great extent, and provided research and operational forecasts for a wide range of applications at a resolution of hundreds of kilometres to hundreds of metres. The Weather Research and Forecasting (WRF) model is a community-based NWP system, which has been extensively used for the prediction of tropical cyclones over the BoB region[7–12]. In spite of the significant improvements achieved in the NWP models, the forecast accuracy for severe weather events such as tropical cyclones still remains a challenge. The poor performance of NWP models can be attributed to the poorly specified model parameter values[13] and inaccuracy in providing the initial conditions[14].

The process of modifying the model parameters to match the model output with that of the observations is known as parameter calibration. The model parameter calibration started as early as 2012 (ref. 15) and is gaining attention lately. Baki et al.[16] calibrated the WRF model parameters for simulations of tropical cyclones over the BoB region and reported considerable improvement in wind speed, precipitation, cyclone track and intensity. In the present study, the calibrated model parameter values reported by Baki et al.[16] are used in the short-term predictions.

Developing appropriate initial conditions for the simulations of tropical cyclones is a challenging task as these cyclones originate over the oceans, where direct *in situ* observations are limited. However, advancements achieved in computational methods and observational instruments have led to the use of superior data assimilation techniques. The available observations can be used in the model to generate accurate initial conditions. Several researchers have utilized the three-dimensional variational (3DVar) assimilation[17–21], four-dimensional variational (4DVar) assimilation[22,23] and hybrid assimilation[24] techniques to

assimilate the *in situ* and satellite observations for predictions of tropical cyclones over the BoB region, and reported considerable improvement in cyclone track and intensity forecasts. The variational technique aims to get the best approximation of the state of the atmospheric system by combining background and observation information and taking into consideration their respective error structures. As a result, an accurate representation of the error covariances is critical in data assimilation systems[25]. Rakesh and Goswami[26] have examined the role of background error statistics generated with global and regional models in 3DVar assimilation for the simulations of tropical cyclones over the north Indian Ocean. They reported that the use of regional background error statistics in 3DVar assimilation improved the cyclone track and intensity predictions significantly. Dhanya and Chandrasekar[27] studied the impact of background error covariance (BEC) in 3DVar assimilation of SAPHIR radiances for the simulation of three tropical cyclones over the BoB region. They examined two covariance options, cv5 and cv6; the simulated cyclones showed high intensity when cv6 was used. Thiruvengadam *et al.*[28] examined the impact of background error statistics of cv5, cv7 and ensemble methods in 3DVar radar data assimilation for the 2015 heavy precipitation event over Chennai. These studies show that the background error covariances affect data assimilation and the use of regional-specific BEC will improve the model forecasts.

So far, studies have used different background error statistics in advanced data assimilation techniques employing the default-built WRF model. However, the performance of the calibration model with the application of multivariate background error statistics is yet to be evaluated. The present study examines the impact of multivariate background error covariances in 3DVar assimilation of conventional and radiance observations using the default and calibration models for simulations of tropical cyclones over the BoB region. To the best of the authors' knowledge, no study has been conducted earlier to examine the impact of background error statistics in 3DVar assimilation with the calibration model.

Model description, calibration set-up and simulation events

In the present study, the WRF model version 3.9.1 was used to perform numerical simulations of seven very severe cyclonic storms over the BoB region[29]. The WRF model is configured with a single domain of 12 km resolution consisting of 250×250 grid points in the horizontal direction (Supplementary Figure 1) and 49 sigma levels in the vertical direction. Based on the study of Kutty *et al.*[24], the 24th-hour forecasts from the National Centers for Environmental Prediction (NCEP) Global Forecast System (GFS) at 0.5° resolution have been used as initial and

boundary conditions to drive the numerical simulations. The WRF model simulations were performed with a time step of 30 sec. The model physics schemes were adapted from Baki *et al.*[16], viz. Kain–Fritsch for cumulus physics[30], MM5 similarity scheme for surface layer physics[31], WRF single-moment 6-class (WSM6) scheme for microphysics[32], rapid radiative transfer model for longwave radiation[33], unified Noah land surface model for land surface physics[34], Dudhia shortwave scheme for shortwave radiation[35] and Yonsei University Scheme (YSU) for planetary boundary-layer physics[36].

Model calibration is a method of improving the performance of a numerical model by tuning the model parameters when comparing with the observations. Baki *et al.*[16] have shown that the calibration of eight sensitive parameters from the seven physics schemes of the WRF model has greatly improved the prediction of 10 m wind speed, precipitation, cyclone track and intensity. With a view to assess the performance of data assimilation with the calibration model, the parameter values obtained by Baki *et al.*[16] were adopted in this study (Supplementary Table 1). Hereafter, the model with default parameter values is referred to as the default model and that with the calibration parameter values as the calibration model.

In the present study, seven tropical cyclones that originated over the BoB region under the very severe cyclonic storm category have been selected for numerical analysis. The selected cyclones originated during the post-monsoon season during the period 2011–18. The India Meteorological Department (IMD) observed tracks of the selected cyclones are shown (Supplementary Figure 1) and Table 1 presents the corresponding landfall times.

Assimilation methodology, background error statistics and data

Description of 3DVar assimilation system

In the present study, the WRF–3DVar system developed using the WRF model was employed for assimilation experiments. The 3DVar system performs minimization of a cost function $J(x)$ to obtain the best estimate of the current state of the atmosphere when provided with the observations. The cost function is defined as[14]

$$J(x) = \frac{1}{2}(x - x_b)^T \mathbf{B}^{-1}(x - x_b)$$

$$+ \frac{1}{2}(y^o - H(x))^T \mathbf{R}^{-1}(y^o - H(x)), \quad (1)$$

where x represents the atmospheric state vector, x_b the first guess of the state, y^o the observational vector and H represents the observational operator which calculates the observation equivalents from the model variables and

Table 1. Overview of the tropical cyclones and corresponding simulation periods

Index	Cyclone	Landfall	Period of spin-up (6 h)	Period of assimilation (four cycles)	Period of free forecast (96 h)
A	VSCS Thane	01Z–02Z 30 December 2011	18Z 25th–00Z 26th	00Z 26th–18Z 26th	18Z 26th–18Z 30th
B	VSCS Leher	0830Z 28 November 2013	00Z 24th–06Z 24th	06Z 24th–00Z 25th	00Z 25th–00Z 29th
C	VSCS Madi	17Z 12 December 2013	06Z 8th–12Z 8th	12Z 8th–06Z 9th	06Z 9th–06Z 13th
D	VSCS Vardah	09Z–10Z 12 December 2016	00Z 8th–06Z 8th	06Z 8th–00Z 9th	00Z 9th–00Z 13th
E	VSCS Titli	00Z 11 October 2018	12Z 6th–18Z 6th	18Z 6th–12Z 7th	12Z 7th–12Z 11th
F	VSCS Hudhud	0630Z 12 October 2014	12Z 7th–18Z 7th	18Z 7th–12Z 8th	12Z 8th–12Z 12th
G	VSCS Gaja	19Z–20Z 15 November 2018	12Z 11th–18Z 11th	18Z 11th–12Z 12th	12Z 12th–12Z 16th

maps them to the observation space. The deviation of the analysis from the first guess is characterized by the BEC matrix **B** and the deviation of the analysis from the observations is characterized by the observation error covariance matrix **R**. Though the equation seems simple, calculating the inverse of **B** with approximately 10^7 degrees of freedom is computationally impractical[37]. To overcome this, one uses the control variable transforms in which the cost function is optimized for the control variables. Consider the control variables **v** defined by the equation $\mathbf{U}\mathbf{v} = x - x_b$ and the transform vector **U** obtained through the background error covariance decomposition as $\mathbf{B} = \mathbf{U}\mathbf{U}^T$. The objective function is transformed into the control variables as follows

$$J(x) = \frac{1}{2}(\mathbf{U}\mathbf{v})^T \mathbf{B}^{-1}(\mathbf{U}\mathbf{v}) + \frac{1}{2}(y^o - H(\mathbf{U}\mathbf{v} + x_b))^T$$
$$\times \mathbf{R}^{-1}(y^o - H(\mathbf{U}\mathbf{v} + x_b)), \tag{2}$$

$$J(x) = \frac{1}{2}\mathbf{v}^T(\mathbf{U}^T\mathbf{B}^{-1}\mathbf{U})\mathbf{v} + \frac{1}{2}(y^o - H(x_b) - \mathbf{H}\mathbf{U}\mathbf{v})^T$$
$$\times \mathbf{R}^{-1}(y^o - H(x_b) - \mathbf{H}\mathbf{U}\mathbf{v}), \tag{3}$$

$$J(x) = \frac{1}{2}\mathbf{v}^T\mathbf{v} + \frac{1}{2}(\mathbf{d} - \mathbf{H}\mathbf{U}\mathbf{v})^T\mathbf{R}^{-1}(\mathbf{d} - \mathbf{H}\mathbf{U}\mathbf{v}), \tag{4}$$

where **d** is the innovation vector that calculates the deviation of observations from the first guess and **H** is the linearized observation operator. The present study uses four control variable transforms – cv3, cv5, cv6 and cv7 – for the assimilation experiments. Each of the transforms utilizes different control variables[29] (Supplementary Table 2). Since the control variables in each transform are different, BEC also needs to be evaluated for each method.

Background error covariance estimation

The cv3 BEC is provided with the original WRF model build source code, which is a global background error that can be used for any regional model. In contrast, the

cv5, cv6 and cv7 covariances are region-specific and thus need to be estimated according to the model domain configuration. The National Meteorological Center (NMC) method, one of the prominent methods developed by Parrish and Derber[38] has been used to estimate BEC by taking the differences between the 24th and 12th-hour forecasts valid at the same time.

$$\mathbf{B} = \overline{(x^b - x^t)(x^b - x^t)^T} \approx \overline{(x^{T+24} - x^{T+12})(x^{T+24} - x^{T+12})^T}, \tag{5}$$

where x^b represents the model atmospheric state, x^t the true atmospheric state, x^{T+24} the 24th hour forecast of the regional model and x^{T+12} represents the 12th hour forecast of the regional model. No assimilation has been performed in calculating the BEC matrices.

Data used for assimilation and model verification

The conventional observations from sources such as land surface, marine surface, radiosonde, pibal and airplane reports from the Worldwide Telecommunications System as well as satellite winds are among the global surface and upper-air observations taken from NCEP in the prepbufr format[39], that are assimilated in the present study. Along with the conventional observations, the radiance observations from various instruments on-board different satellites such as Advanced Microwave Sounding Unit-A (AMSU-A), Microwave Humidity Sounder (MHS), High resolution Infra-Red Sounder-4 (HIRS4), Infrared Atmospheric Sounding Interferometer (IASI), Special Sensor Microwave/Imager (SSM/I) and Atmospheric Infra-Red Sounder (AIRS) have also been assimilated whenever available[40]. More details regarding the assimilated observations are presented in the Supplementary Table 3.

The IMD observations of cyclone track and intensity have been utilized to validate the model forecasts. The Integrated Multi-satellitE Retrievals for GPM (IMERG) dataset available at $0.1° \times 0.1°$ resolution was employed to validate the precipitation forecasts[41]. The Indian Monsoon Data Assimilation and Analysis (IMDAA) data available at $0.12° \times 0.12°$ resolution was used to validate wind speed[42].

Table 2. Details of numerical experiments performed for each cyclone

Experiment	Description
Default	Simulations performed with the default model without data assimilation
Default + cv3_assimilation	Simulations performed with the default model and data assimilation using cv3 BEC
Default + cv5 assimilation	Simulations performed with the default model and data assimilation using cv5 BEC
Default + cv6 assimilation	Simulations performed with the default model and data assimilation using cv6 BEC
Default + cv7 assimilation	Simulations performed with the default model and data assimilation using cv7 BEC
Calibration	Simulations performed with the calibration model without data assimilation
Calibration + cv3 assimilation	Simulations performed with the calibration model and data assimilation using cv3 BEC
Calibration + cv5 assimilation	Simulations performed with the calibration model and data assimilation using cv5 BEC
Calibration + cv6 assimilation	Simulations performed with the calibration model and data assimilation using cv6 BEC
Calibration + cv7 assimilation	Simulations performed with the calibration model and data assimilation using cv7 BEC

Design of experiments

The objective of the present study was to assess the impact of multivariate BEC assimilation using the conventional and radiance observations with the default and calibration models. For this, BEC corresponding to cv5, cv6 and cv7 need to be estimated before hand, whereas BEC of cv3 is provided along with the WRF–3DVar build system. As mentioned earlier, the NMC method has been adopted to estimate BEC of cv5, cv6 and cv7, which requires the 24th and 12th-hour model forecasts that are valid at the same time. The tropical cyclones have been selected for the experiments such that they all occurred in the post-monsoon (October–December) period between 2011 and 2018. To calculate BEC, a two-month period from 15 October to 15 December 2016 was chosen to represent the climatology of the post-monsoon period[43,44]. The 24 and 12-h forecasts using the default and calibration models were performed over the selected period. Using the NMC method, BEC values of cv5, cv6 and cv7 were estimated for the default and calibration models.

Once the BEC values were estimated, a total of 10 experiments were conducted for the simulations of the seven tropical cyclones (Table 2). The domain configuration and resolution used in the data assimilation experiments were the same as that of the WRF model simulations. It has been assumed that the observations are statistically independent of one another. Thus, the observational error covariance matrix is diagonal. The observations were thinned with a threshold of 30 km before assimilating. The Supplementary Table 4 presents the total number of conventional and radiance observations that have been assimilated during the last assimilation cycle, for all the cyclones. To illustrate the distribution of conventional observations, a scatter plot of the same for cyclone Vardah is presented in the Supplementary Figure 2. Table 1 shows the duration of simulation of each cyclone for the experiments. Each assimilation experiment has been initialized with the model forecast simulated for the spin-up period and four assimilation cycles were carried out. The assimilation experiments were conducted in a continuous mode, such that the wrfout files from the last 6 h of simulations were provided as background or first guess for the next 6 h of the assimilation cycle. After the assimilation cycles, a free forecast of 96 h was carried out for all the experiments, which implies the assimilation experiments were simulated for a total of 126 h, whereas experiments without assimilation were simulated for a total of 96 h. Finally, a total of 70 numerical simulations were performed in the present study.

The performance of the model forecasts was validated against the observations for the variables such as wind speed at 10 m height, precipitation, cyclone tracks and the central sea level pressure (CSLP). The simulated variables were extracted at 6 h intervals, and the root means square error (RMSE) between the model simulations and observations was considered as the verification metric.

$$\text{RMSE} = \sqrt{\frac{\left[\sum_{k=1}^{K}\sum_{j=1}^{J}\sum_{i=1}^{I}(\text{sim}_{ijkl} - \text{obs}_{ijkl})^2\right]}{I \times J \times K}}, \quad (6)$$

$$\text{RMSE}_{\text{Overall}} = \sqrt{\frac{\sum_{L=1}^{7}\text{RMSE}_L^2}{7}}, \quad (7)$$

$$\text{Gain (or) loss\%} = \frac{\text{RMSE}_{\text{default}} - \text{RMSE}}{\text{RMSE}_{\text{default}}} \times 100, \quad (8)$$

where I and J represent the number of grid points in horizontal space, K the number of time intervals, L the number of cyclones, sim the simulated value and obs is the observed value. Equation (6) was used to estimate RMSE values of each variable for the individual cyclones, whereas eq. (7) was used to estimate the overall RMSE of all the cyclones together. The RMSE values of each experiment were compared with that of the default experiment, and the gain or loss per cent was estimated using eq. (8). In addition to the RMSE value, visualization of the spatial structures of the variables was also done to assess the impact of assimilation in combination with model calibration.

Table 3. Root mean square error (RMSE) values of 10 m wind speed (m/s) obtained with all the experiments for the simulations of selected events

Experiment	Thane	Leher	Madi	Vardah	Titli	Hudhud	Gaja	Overall
Default	2.518392	3.325867	2.829489	1.943036	3.769595	5.206273	2.324268	3.2929
Default + cv3	2.797652	3.307635	2.798626	1.809836	3.924218	3.621974	2.285098	3.0146
	(−11.09%)	(0.55%)	(1.09%)	(6.86%)	(−4.1%)	(30.43%)	(1.69%)	(8.45%)
Default + cv5	2.702016	3.054904	2.74938	1.948609	3.629611	4.765588	2.262552	3.1395
	(−7.29%)	(8.15%)	(2.83%)	(−0.29%)	(3.71%)	(8.46%)	(2.66%)	(4.66%)
Default + cv6	2.620374	3.125547	2.697757	2.029305	3.776702	4.553418	2.29121	3.1231
	(−4.05%)	(6.02%)	(4.66%)	(−4.44%)	(−0.19%)	(12.54%)	(1.42%)	(5.16%)
Default + cv7	2.762355	3.0193	2.868379	1.796751	3.739866	5.310015	2.251376	3.2832
	(−9.69%)	(9.22%)	(−1.37%)	(7.53%)	(0.79%)	(−1.99%)	(3.14%)	(0.29%)
Calibration	2.402599	3.155955	2.536693	1.943326	3.218292	4.363365	2.403766	2.9549
	(4.6%)	(5.11%)	(10.35%)	(−0.01%)	(14.62%)	(16.19%)	(−3.42%)	(10.26%)
Calibration + cv3	3.113613	3.073021	2.516863	1.720061	3.136423	3.54398	2.300585	2.8315
	(−23.63%)	(7.6%)	(11.05%)	(11.48%)	(16.8%)	(31.93%)	(1.02%)	(14.01%)
Calibration + cv5	2.764063	3.101451	2.546504	1.785002	3.101872	3.805947	2.424715	2.8515
	(−9.76%)	(6.75%)	(10%)	(8.13%)	(17.71%)	(26.9%)	(−4.32%)	(13.4%)
Calibration + cv6	2.616491	3.245237	2.527597	1.789947	3.137858	3.158915	2.337378	2.7323
	(−3.9%)	(2.42%)	(10.67%)	(7.88%)	(16.76%)	(39.32%)	(−0.56%)	(17.02%)
Calibration + cv7	2.655447	3.180668	2.57116	1.770802	3.088611	4.298706	2.29033	2.9321
	(−5.44%)	(4.37%)	(9.13%)	(8.86%)	(18.07%)	(17.43%)	(1.46%)	(10.96%)

The percentage value indicates the reduction in RMSE value of the corresponding experiment when compared to the default experiment.

Once the performance of the assimilation experiments and the calibration model was evaluated, the best experimental set-up was used to simulate the recent cyclone Gulab to represent the operational forecast. This cyclone occurred during the end of the monsoon of 2021, under the category of a cyclonic storm and brought heavy rainfall over the Visakhapatnam coast during landfall. The model simulations were initialized at 1800 UTC of 24 September 2021 and simulated till 0000 UTC of 27 September 2021, with the same experimental set-up. The cyclone track and intensity were compared with observations, and the robustness of the best experimental set-up was verified.

Results and discussion

In this section, results from the simulation experiments mentioned in Table 2 are discussed in detail. The RMSE values of the simulated model variables such as 10 m wind speed, precipitation, cyclone track and intensity were evaluated against the observations for all the events using eq. (6) (Tables 3–6). The percentage values shown in each table represent the gain or loss of each experiment when compared to the default experiment and have been calculated using eq. (8). The time evolution of the cyclone tracks and their intensities are presented in Figure 1. Apart from the RMSE values, the spatial structures of essential variables such as precipitation, wind speed, relative humidity, mean ascent, and potential vorticity were also examined for cyclones Vardah and Hudhud (Figures 2–6 and Supplementary Figures 3–7). With the obtained best experimental set-up, cyclone Gulab was simulated and the model forecasts were compared with the observations (Supplementary Figure 8).

Assessment of assimilation experiments with the default model

Table 3 presents a comparison of RMSE values of the 10 m wind speed for simulations of seven tropical cyclones obtained by the assimilation experiments with the default model. The results show that the assimilation indeed improved the 10 m wind speed forecast, and the improvement varies with the adopted BEC. The cv3 assimilation experiments showed a reduction in the RMSE value ranging from 0.55% for cyclone Leher to 30.43% for cyclone Hudhud, and an overall reduction of 8.45%. Even though the assimilation increased the RMSE for cyclones Thane and Titli, a good overall reduction was seen with cv3 assimilation. The overall reduction in the RMSE values obtained with the cv5, cv6 and cv7 assimilation experiments were 4.66%, 5.16% and 0.30% respectively. The cv7 assimilation experiments yielded the least reduction and increased the RMSE values for cyclones Thane, Madi and Hudhud. These results indicate that the 3DVar assimilation of conventional and radiance observations with the cv3 BEC yields a higher reduction of RMSE in the 10 m wind speed compared to the remaining BEC experiments.

Similar to Table 3, a comparison of precipitation RMSE values is shown in Table 4 for the assimilation experiments

Table 4. RMSE values of precipitation (mm/day) obtained with all the experiments for the simulations of selected events

Experiment	Thane	Leher	Madi	Vardah	Titli	Hudhud	Gaja	Overall
Default	5.646609	8.564379	6.318636	7.121049	9.334765	12.21196	6.912598	8.2801
Default + cv3	6.185905	7.76018	5.795774	7.362394	9.209872	11.28624	6.937319	7.9876
	(−9.55%)	(9.39%)	(8.27%)	(−3.39%)	(1.34%)	(7.58%)	(−0.36%)	(3.53%)
Default + cv5	6.694844	7.659243	5.688378	7.427496	9.070935	10.6987	6.222384	7.8054
	(−18.56%)	(10.57%)	(9.97%)	(−4.3%)	(2.83%)	(12.39%)	(9.98%)	(5.73%)
Default + cv6	6.371046	7.221573	5.613238	7.675553	9.277752	10.3808	6.581964	7.749
	(−12.83%)	(15.68%)	(11.16%)	(−7.79%)	(0.61%)	(14.99%)	(4.78%)	(6.41%)
Default + cv7	6.877731	8.030886	6.153779	7.903815	9.607932	11.94079	6.425834	8.352300
	(−21.8%)	(6.23%)	(2.61%)	(−10.99%)	(−2.93%)	(2.22%)	(7.04%)	(−0.87%)
Calibration	5.455867	8.092178	5.792993	6.878628	8.552558	11.67931	6.60843	7.8317
	(3.38%)	(5.51%)	(8.32%)	(3.4%)	(8.38%)	(4.36%)	(4.4%)	(5.42%)
Calibration + cv3	6.728626	7.194079	5.424164	6.805307	8.268903	10.37094	5.949652	7.4075
	(−19.16%)	(16%)	(14.16%)	(4.43%)	(11.42%)	(15.08%)	(13.93%)	(10.54%)
Calibration + cv5	6.208499	7.456908	5.784012	7.224377	8.300693	10.74274	5.51987	7.5078
	(−9.95%)	(12.93%)	(8.46%)	(−1.45%)	(11.08%)	(12.03%)	(20.15%)	(9.33%)
Calibration + cv6	5.875585	7.703748	5.563658	7.166390	8.346104	10.10776	5.558631	7.3573
	(−4.06%)	(10.05%)	(11.95%)	(−0.64%)	(10.59%)	(17.23%)	(19.59%)	(11.14%)
Calibration + cv7	6.171494	8.484735	5.912846	7.506289	8.4571	10.90779	5.996292	7.8179
	(−9.3%)	(0.93%)	(6.42%)	(−5.41%)	(9.4%)	(10.68%)	(13.26%)	(5.58%)

The percentage value indicates the reduction in RMSE value of the corresponding experiment when compared to the default experiment.

Table 5. RMSE values of cyclone track (km) obtained with all the experiments for the simulations of selected events

Experiment	Thane	Leher	Madi	Vardah	Titli	Hudhud	Gaja	Overall
Default	177.8693	290.5611	71.1377	221.0327	351.6559	176.0321	240.616	233.7656
Default + cv3	147.0173	343.2250	226.3518	76.5605	223.4351	223.3987	199.219	219.0996
	(17.35%)	(−18.12%)	(−218.1%)	(65.36%)	(36.46%)	(−26.91%)	(17.2%)	(6.27%)
Default + cv5	338.8340	189.2105	100.7656	107.5682	308.5161	113.8616	196.6394	213.524
	(−90.5%)	(34.88%)	(−41.6%)	(51.33%)	(12.27%)	(35.32%)	(18.28%)	(8.66%)
Default + cv6	342.9835	186.7771	105.1982	97.3254	253.1801	81.0791	221.7702	204.5616
	(−92.83%)	(35.72%)	(−47.8%)	(55.97%)	(28%)	(53.94%)	(7.83%)	(12.49%)
Default + cv7	424.2700	167.9303	113.7120	138.9702	345.9909	149.1574	145.1022	240.0778
	(−138.5%)	(42.2%)	(−59.8%)	(37.13%)	(1.61%)	(15.27%)	(39.7%)	(−2.7%)
Calibration	196.2511	236.3334	101.6199	192.4481	292.1468	157.6208	272.4421	215.8537
	(−10.33%)	(18.66%)	(−42.8%)	(12.93%)	(16.92%)	(10.46%)	(−13.23%)	(7.66%)
Calibration + cv3	223.3174	276.4801	186.5811	96.1979	364.2464	166.2352	142.2946	223.9055
	(−25.55%)	(4.85%)	(−162.2%)	(56.48%)	(−3.58%)	(5.57%)	(40.86%)	(4.22%)
Calibration + cv5	130.3011	123.9356	196.4045	98.7521	177.6817	112.4912	174.7763	149.0143
	(26.74%)	(57.35%)	(−176.0%)	(55.32%)	(49.47%)	(36.1%)	(27.36%)	(36.25%)
Calibration + cv6	99.5716	88.1652	153.8382	79.9539	215.2142	104.4018	154.9971	135.7452
	(44.02%)	(69.66%)	(−116.2%)	(63.83%)	(38.8%)	(40.69%)	(35.58%)	(41.93%)
Calibration + cv7	165.0091	131.3842	184.1514	140.4442	164.4443	99.763	141.6624	148.8954
	(7.23%)	(54.78%)	(−158.8%)	(36.46%)	(53.24%)	(43.33%)	(41.13%)	(36.31%)

The percentage value indicates the reduction in RMSE value of the corresponding experiment when compared to the default experiment.

with the default model. The RMSE values indicate that the assimilation experiments with cv3, cv5 and cv6 yield an overall reduction of 3.63%, 5.73% and 6.41% respectively. In contrast, the cv7 assimilation experiments deteriorated the precipitation forecast with an increase in the RMSE value of 0.87%. The RMSE values are increased for two cyclones in the cv6 and cv5 assimilation experiments, whereas they increased for three cyclones in the cv3 assimilation experiments. These assimilation experiments show a general trend of RMSE reduction for cv5 and cv6 experiments, with cv6 having the highest reduction. Table 5 shows a similar comparison to that of Table 3, but for the cyclone track RMSE. Here too, the cv6 assimilation experiments yield a higher reduction of 12.49% compared to the remaining experiments, and the cv7 assimilation experiments show an increase in the RMSE of 2.70%. Similar to precipitation, the cv5 and cv6 experiments show a general trend of RMSE reduction for five

Table 6. RMSE values of central sea level pressure (CSLP) (hPa) obtained with all the experiments for the simulations of selected events

Experiments	Thane	Leher	Madi	Vardah	Titli	Hudhud	Gaja	Overall
Default	17.9413	12.14526	8.821471	12.66976	5.555528	18.34348	15.70185	13.7406
Default + cv3	13.69911	10.28307	2.819863	5.743091	9.249365	7.727607	11.05876	9.2729
	(23.64%)	(15.33%)	(68.03%)	(54.67%)	(−66.49%)	(57.87%)	(29.57%)	(32.51%)
Default + cv5	19.53979	7.098686	2.129566	9.446058	7.796382	16.92346	11.03969	11.9225
	(−8.91%)	(41.55%)	(75.86%)	(25.44%)	(−40.34%)	(7.74%)	(29.69%)	(13.23%)
Default + cv6	19.99536	7.744434	1.929001	7.138514	11.40703	13.75173	11.37618	11.7298
	(−11.45%)	(36.23%)	(78.13%)	(43.66%)	(−105.3%)	(25.03%)	(27.55%)	(14.63%)
Default + cv7	21.42595	3.35923	3.02491	8.254278	9.896218	23.14418	10.41792	13.5739
	(−19.42%)	(72.34%)	(65.71%)	(34.85%)	(−78.13%)	(−26.17%)	(33.65%)	(1.21%)
Calibration	18.24191	8.613636	5.024959	12.30818	10.72628	18.08974	14.55525	13.298
	(−1.68%)	(29.08%)	(43.04%)	(2.85%)	(−93.07%)	(1.38%)	(7.3%)	(3.22%)
Calibration + cv3	10.78801	10.41273	4.66364	8.200301	14.92930	9.370005	10.94832	10.3119
	(39.87%)	(14.27%)	(47.13%)	(35.28%)	(−168.7%)	(48.92%)	(30.27%)	(24.95%)
Calibration + cv5	12.13384	6.141888	3.177584	7.916072	14.21136	17.78974	12.34541	11.5174
	(32.37%)	(49.43%)	(63.98%)	(37.52%)	(−155.8%)	(3.02%)	(21.38%)	(16.18%)
Calibration + cv6	13.56174	6.131842	3.404819	8.549292	13.64922	10.778	11.17147	10.2363
	(24.41%)	(49.51%)	(61.4%)	(32.52%)	(−145.6%)	(41.24%)	(28.85%)	(25.5%)
Calibration + cv7	14.23129	8.717669	4.61051	11.12899	14.84735	23.86141	10.44912	13.74580
	(20.68%)	(28.22%)	(47.74%)	(12.16%)	(−167.2%)	(−30.08%)	(33.45%)	(−0.04%)

The percentage value indicates the reduction in RMSE value of the corresponding experiment when compared to the default experiment.

cyclones, whereas the cv3 experiments show a reduction for four cyclones. Though the cv7 experiments also show a reduction for five cyclones, the RMSE value for cyclone Thane is very large, which leads to an increase in the overall RMSE.

Table 6 shows the RMSE comparison of cyclone intensity in terms of Central sea level pressure (CSLP), for the assimilation experiments with the default model. The cv3 assimilation experiments show the highest reduction of 32.51%, improving the intensity forecast for all cyclones, except Titli. The assimilation experiments of cv5 and cv6 also show a general trend of cyclone track forecast improvement with an overall RMSE reduction of 13.23% and 14.63% respectively. In contrast, the experiments of cv7 show an RMSE increase for three cyclones, and the overall RMSE reduction is also less. These results indicate that the assimilation experiments with cv3, cv5 and cv6 BEC values generally improve the model forecasts of 10 m wind speed, precipitation, cyclone track and intensity.

Assessment of calibration model

So far, we have examined the experiments conducted with the default model. However, the robustness of the calibration model must also be evaluated before examining the impact of the assimilation experiments conducted with it. For this, the RMSE values of 10 m wind speed, precipitation, cyclone track and intensity that are obtained with the calibration experiments were evaluated (Tables 3–6). The results indicate a general trend of RMSE reduction for all the variables, with an overall reduction of 10.27% for 10 m wind speed, 5.42% for precipitation,

7.66% for cyclone track and 3.22% for CSLP. The RMSE values of precipitation had reduced for all the cyclones, ranging from 8.38% for the cyclone Titli to 3.38% for cyclone Thane. Similarly, the RMSE values of 10 m wind speed had reduced for five cyclones, ranging from 16.19% for cyclone Hudhud and 4.60% for cyclone Thane. The RMSE values of the cyclone track had reduced for four cyclones and RMSE values of the intensities had reduced for five cyclones. The calibration methodology adopted by Baki et al.[16] minimizes the 10 m wind speed and precipitation forecasts simultaneously. Thus, the calibration experiments showed a good improvement for the 10 m wind speed and precipitation forecasts, whereas the improvements were seen in the cyclone track and the CSLP forecasts were considered to be the secondary gain. Baki et al.[16] used the NCEP FNL data at 1° resolution as the initial and boundary conditions for the numerical simulations. In contrast, the present study uses the NCEP-GFS data at 0.5° resolution as initial and boundary conditions. Thus, the difference in the model forecasts post the calibration experiments is attributed to the difference in the adopted initial and boundary conditions. Overall, the calibration model is seen to be robust in improving the model forecasts.

Assessment of assimilation experiments with the calibration model

Table 3 presents a comparison of RMSE values of the 10 m wind speed for simulations of seven tropical cyclones obtained by the assimilation experiments using the calibration model. The results show that assimilation with the
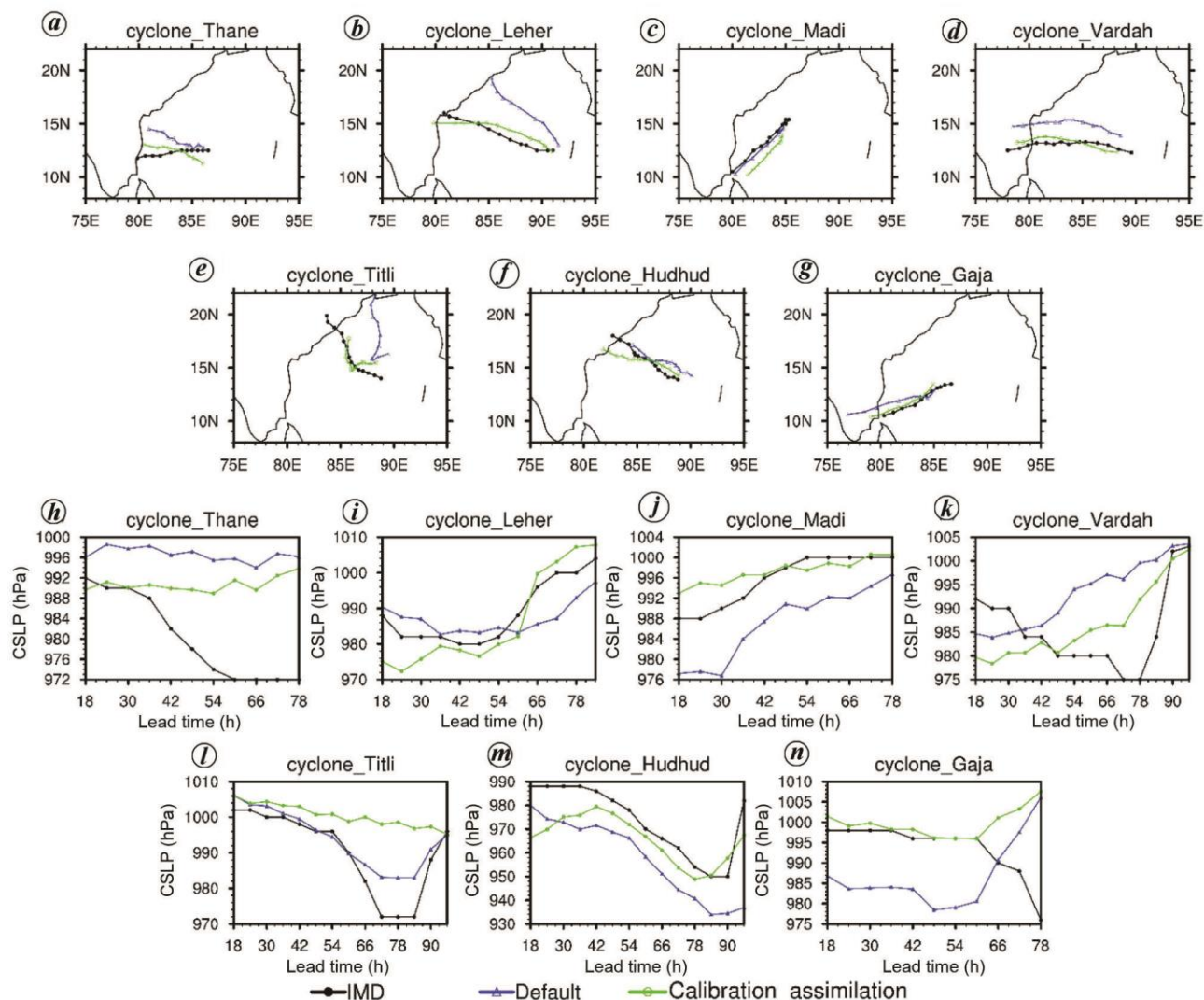
Figure 1. Illustration of (*a*–*g*) cyclone tracks and (*h*–*n*) time evolution of intensities, simulated with the default model without assimilation and calibration model with assimilation, in comparison with the IMD observations, for the simulations of (*a*, *h*) cyclone Thane; (*b*, *i*) cyclone Leher; (*c*, *j*) cyclone Madi; (*d*, *k*) cyclone Vardah; (*e*, *l*) cyclone Titli; (*f*, *m*) cyclone Hudhud; (*g*, *n*) cyclone Gaja.

calibration model shows a general trend of improvement for the 10 m wind speed forecast. The cv6 assimilation experiment shows the highest overall RMSE reduction of 17.02%, whereas the assimilation experiments with cv3, cv5 and cv7 show 14.01%, 13.4% and 10.96% reduction respectively. The cv6 assimilation experiments deteriorated the 10 m wind speed forecast slightly for cyclones Thane and Gaja with an RMSE increase of –3.9% and –0.56% respectively, whereas the cv5 experiments showed an RMSE increase of –9.76% and –4.32% respectively for the two cyclones. The cv3 assimilation experiments deteriorated the forecast of 10 m wind speed for cyclone Thane with an RMSE increase of –23.63%, whereas the cv7 experiments showed an RMSE increase of 5.44% for the cyclone. Though the cv6 assimilation experiments deteriorated the forecast of the two cyclones, their reduction was minimal, leading to the highest overall gain.

Table 4 presents the RMSE values of precipitation obtained from the assimilation experiments with the calibration model. The results show that the cv3 assimilation experiments improved the precipitation forecast for all the cyclones, with an overall RMSE reduction of 10.54%, except cyclone Thane, for which the RMSE increased by 19.16%. The assimilation experiments of cv5, cv6 and cv7 showed an overall RMSE reduction of 9.33%, 11.14% and 5.58% respectively, but deteriorated the precipitation forecast for cyclones Thane and Vardah. The cv6 assimilation experiment showed the least loss for the two cyclones, leading to the highest overall gain compared to the remaining experiments.

Similar to the 10 m wind speed and precipitation, Table 5 presents the RMSE values of the cyclone track obtained from the assimilation experiments with the calibration model. The results show that the cv3 assimilation
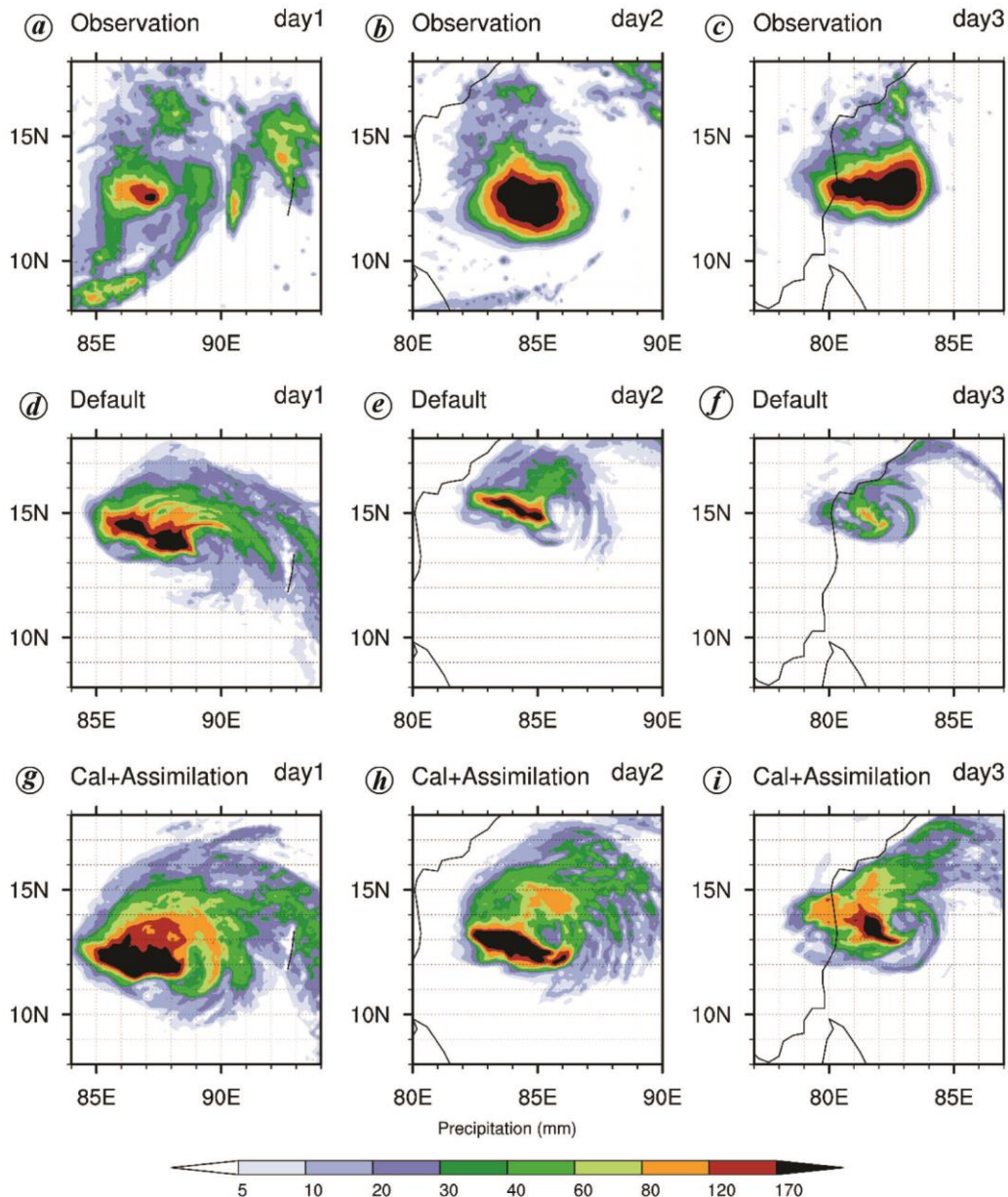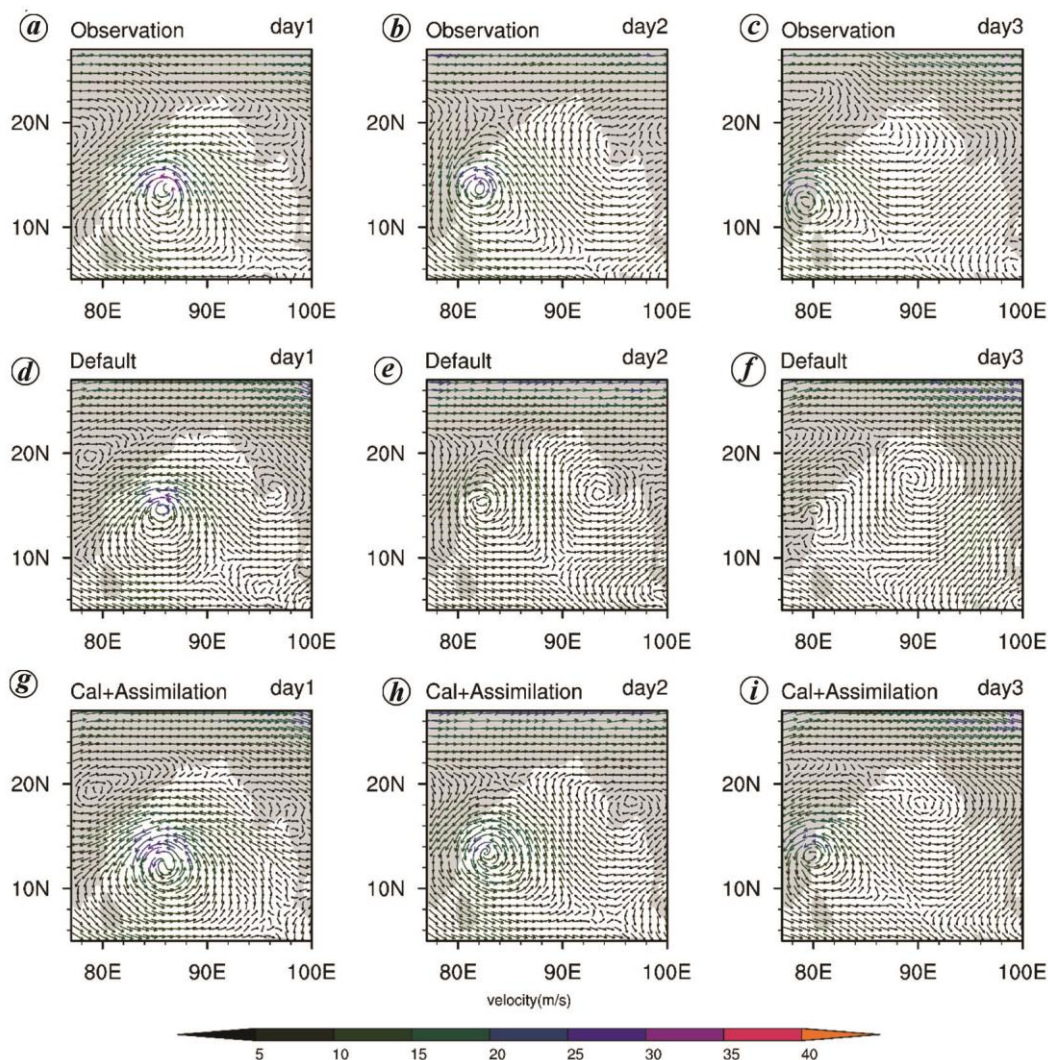
Figure 2. Illustration of daily precipitation shown for the simulation of cyclone Vardah (*a–c*) depict observations from days 1–3 respectively; (*d–f*) depict simulations using the default model without assimilation, and (*g–i*) depict simulations using the calibrated model with assimilation.

experiments deteriorated the track forecast for cyclones Thane, Madi, and Titli, leading to the least overall RMSE reduction of 4.22% compared to the remaining experiments. The cv5, cv6 and cv7 assimilation experiments showed a consistent RMSE reduction for all the cyclones with an overall reduction of 36.25%, 41.93%, 36.31% respectively, but deteriorated the track forecast for cyclone Madi. Among all the experiments, the cv6 experiments had the highest overall RMSE reduction.

Finally, Table 6 presents the RMSE values of cyclone intensity in terms of CSLP obtained from the assimilation experiments with the calibration model. The results show that the assimilation experiments of cv3, cv5 and cv6

indeed improve the cyclone intensity forecast for all the cyclones, except cyclone Titli, with an overall RMSE reduction of 24.95%, 16.18% and 25.5% respectively. In contrast, the cv7 assimilation experiments deteriorated the intensity forecast for cyclones Titli and Hudhud, leading to the overall deterioration. Among the experiments, cv6 showed the highest RMSE reduction, whereas the cv7 showed no improvement.

The results from the RMSE comparison of 10 m wind speed, precipitation, cyclone track, and intensity indicate that the assimilation experiments with the calibration model show consistent improvement compared to the assimilation experiments with the default model, implying

Figure 3. Illustration of winds at 500 hPa level for the simulation of cyclone Vardah (*a–c*) depict observations at the end of days 1–3 respectively; (*d–f*) depict simulations using the default model without assimilation, and (*g–i*) depict simulations using the calibrated model with assimilation.

that assimilation with calibration indeed improves the forecasts. The cv6 assimilation experiments with the calibration model showed the greatest improvement for all the variables compared to the remaining experiments, implying that this is the best experimental set-up. Figure 1 shows the time evolution of cyclone tracks and the corresponding CSLP simulated with the default experiments and the best experiment, and compared with the IMD observations for all the cyclones. The figure shows that cyclone tracks simulated with the best configuration closely followed the IMD observations for all cyclones, except the cyclone Madi, which is again confirmed by Table 5. However, for cyclone Hudhud, the best configuration closely followed the observed track till the end of the second day and deviated thereafter, whereas the default experiments failed to simulate landfall. In contrast, the tracks from the default experiments showed large deviation from the observations for cyclones Thane, Leher, Vardah and Titli, which can be confirmed by Table 3. Figure 1 shows a similar comparison of the time evolution of cyclone intensity in terms of CSLP for all the cyclones. Except for cyclone Titli, the best experiments simulated the time evolution of CSLP quite closely to that of the observations for all the cyclones. The default experiments underestimated the intensity for cyclones Thane and Vardah, whereas they overestimated the intensity for cyclones Madi, Hudhud and Gaja. In contrast, the best experiments underestimated the intensity for cyclones Thane, Vardah and Gaja, but performed better than the default experiments. These results indicate that the assimilation of conventional and radiance observations with the cv6 BEC using the calibration model results in better performance than experiments using the default model without assimilation.

Discussion on model forecasts of cyclone Thane

For cyclone Thane, the RMSE values of surface wind speed and precipitation reveal that the calibration model
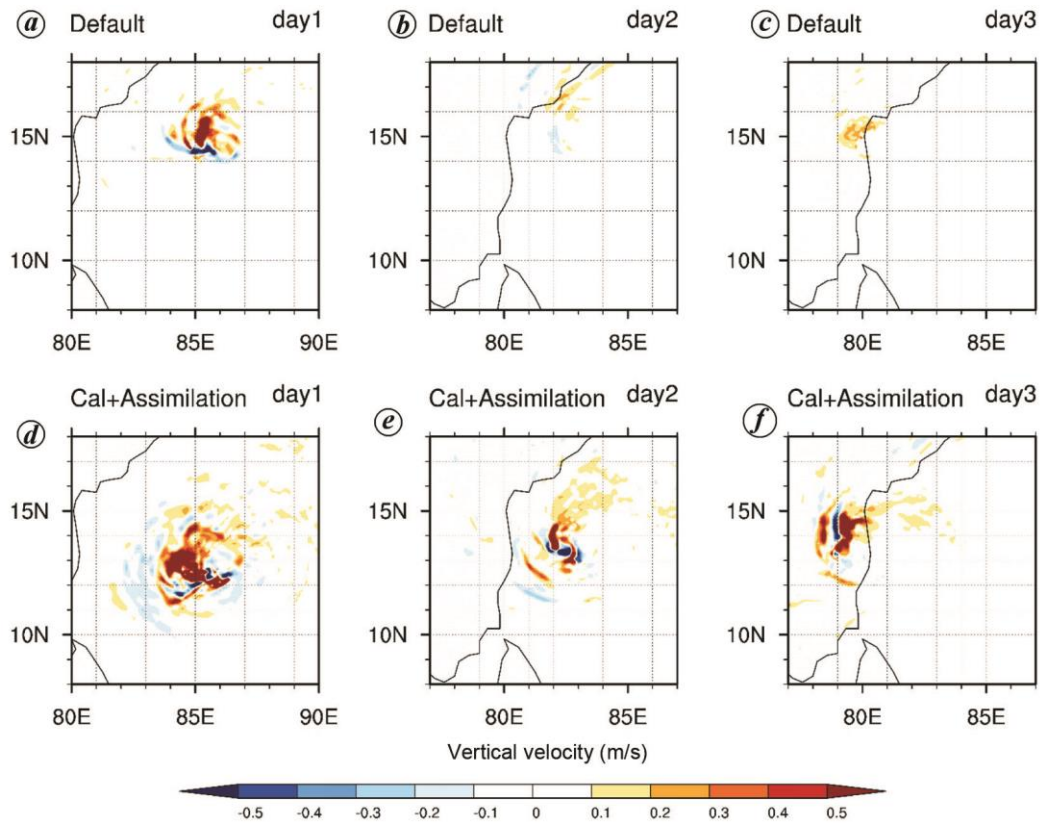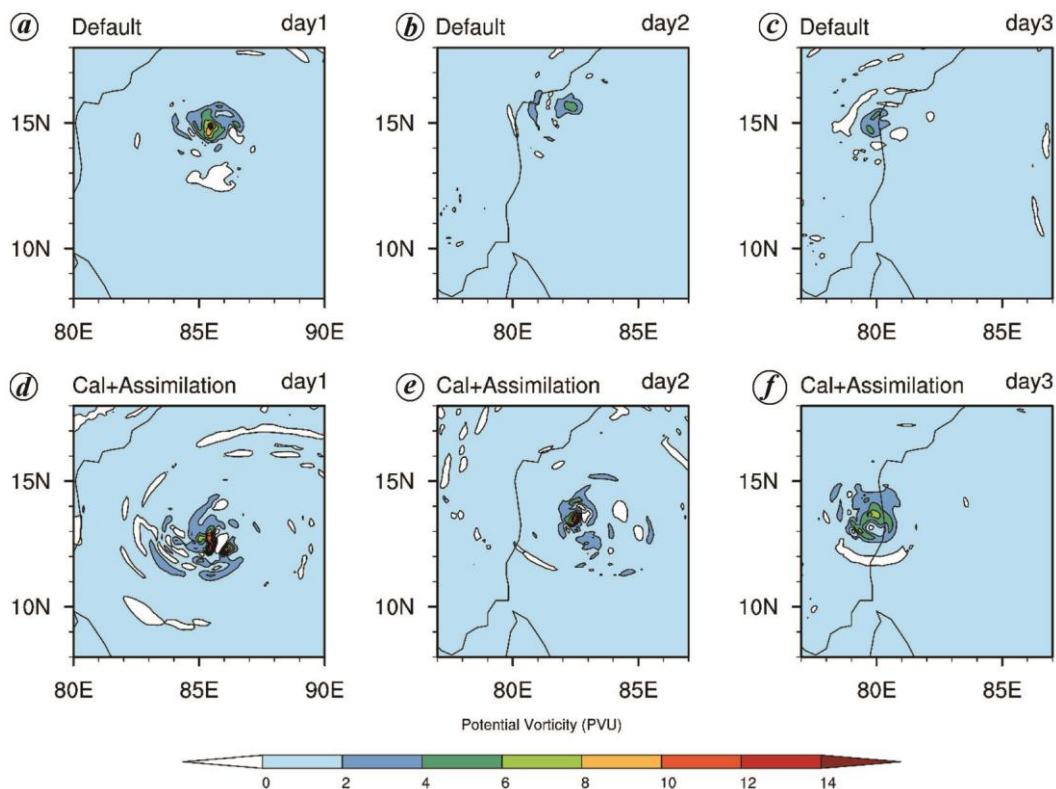
Figure 4. For the simulation of cyclone Vardah, the 500 hPa level vertical velocity (mean ascent) at the end of days 1, 2 and 3 are illustrated. Simulations using the default model without assimilation are shown in (*a–c*), while simulations using the calibrated model with assimilation are shown in (*d–f*).

improved the forecasts by 4.6% and 3.38% respectively, compared to the default model, indicating that the calibrated model is robust for surface wind speed and precipitation forecasts. In contrast, the default and calibration models have underestimated the cyclone intensity and have shown a large deviation in the cyclone track compared to the IMD observations. Similar results have been reported by other researchers[20,21], showing that the WRF model simulations with the GFS initial conditions have landfall over the Machilipatnam coast, with an underestimated cyclone intensity. These results indicate that the GFS initial and boundary conditions themselves have an error, which further deteriorates the forecasts with the calibration model. Chandrasekhar and Balaji[11] have reported that the 3DVar assimilation of conventional and radiance observations with cv3 BEC matrix improved the track forecasts, whereas it deteriorated the wind speed forecasts. The same has been observed in Default + cv3 experiments in the present study, indicating that the assimilation failed to improve the model forecasts of some variables. In contrast, the assimilation experiments of the calibration model with the cv6 BEC matrix have improved the model forecasts of all variables compared to the same assimilation configuration with the default model, indicating that the calibration and assimilation with the cv6 BEC matrix positively contributed to the model forecasts.

Verification of model forecasts for cyclone Vardah

The impact of the assimilation using the calibration model in combination with cv6 BEC on atmospheric variables, namely precipitation, surface wind speed, vertical velocity, potential vorticity and relative humidity were examined for cyclone Vardah (Figures 2–6). The IMERG dataset was used for precipitation verification, whereas the IMDAA dataset was used for verification of the remaining variables. The spatial distribution of 24 h accumulated precipitation at the end of the first, second and third days shown in Figure 2, indicates that the default experiment and best experimental set-up have overestimated precipitation at the end of the first day, whereas it has been underestimated at the end of the second and third days. Though the intensities are far less than those observed, the best experimental set-up shows relatively better performance than the default experiment at the end of the second and third days. However, overestimation of precipitation at the end of the first day is large enough to suppress the improvement on the second and third days, which leads to the overall increase in RMSE.

Figure 3 shows a comparison of the velocity field at 500 hPa level obtained from the best experiment and default experiment. In comparison with the observations, the default experiment simulated a less intense cyclonic

Figure 5. For the simulation of cyclone Vardah, the 500 hPa level potential vorticity at the end of days 1, 2 and 3 are illustrated. Simulations using the default model without assimilation are shown in (*a*–*c*), while simulations using the calibrated model with assimilation are shown in (*d*–*f*).

circulation at the end of the first and second days, and an unorganized circulation was seen at the end of the third day. In contrast, the best experimental set-up simulated a more intense cyclonic circulation at the end of the first day and less intense circulations at the end of the second and third days compared to the observations. This can also be seen in Figure 1 *k*, where the observations lie between default and best experiments at the end of the first day. A comparison of velocity and precipitation shows that the assimilation of conventional and radiance observations using the calibration model in combination with cv6 BEC improved the precipitation forecast.

An inter-comparison of the prominent meteorological variables such as mean ascent, potential vorticity and relative humidity was carried out between the default and best experimental set-up to further examine the impact of assimilation. The mean ascent (vertical velocity in the upward direction) at 500 hPa level was used as a proxy for the deep convection, which directly correlated to the intensity of a tropical cyclone[45–47]. Figure 4 shows that the best experimental set-up resulted in huge spatial coverage of mean ascent with higher values at the end of days 1, 2 and 3, when compared to the default experiments. This analogy is strengthened by Figure 1 *k*, where the cyclone intensity produced by the best experimental set-up is much higher than the default experiment at the end of days 1, 2 and 3. Figure 5 shows the potential vorticity at the end of days 1, 2 and 3, which indicates that the

best experimental set-up simulated more localized potential disturbances compared to the default experiment. According to Ma and Tan *et al.*[48] and Baki *et al.*[12] the energy disturbances that are not consumed by convection may contribute to cyclone intensification. From Figure 5, it is evident that the best experimental set-up simulated higher intensity at the end of days 1, 2 and 3, compared to the default experiment. Relative humidity is an important factor for rapid intensification and helps in the attainment of maximum intensity[49–51]. The spatial distribution of relative humidity shown in Figure 6 reveals that the best experimental set-up simulated huge spatial coverage with higher values at the end of days 1, 2 and 3, indicating that the best experimental set-up produced higher cyclone intensities compared to the default experiment. These results indicate that the assimilation of conventional and radiance observations using the calibration model in combination with cv6 improved the cyclone intensity forecast through improvement of mean ascent, potential vorticity and relative humidity forecasts.

Verification of model forecasts for cyclone Hudhud

Similar to cyclone Vardah, the impact of the assimilation using the calibration model in combination with the cv6 BEC on atmospheric variables were examined for cyclone Hudhud (Supplementary Figures 3–7). The spatial patterns of precipitation show that the default and the best
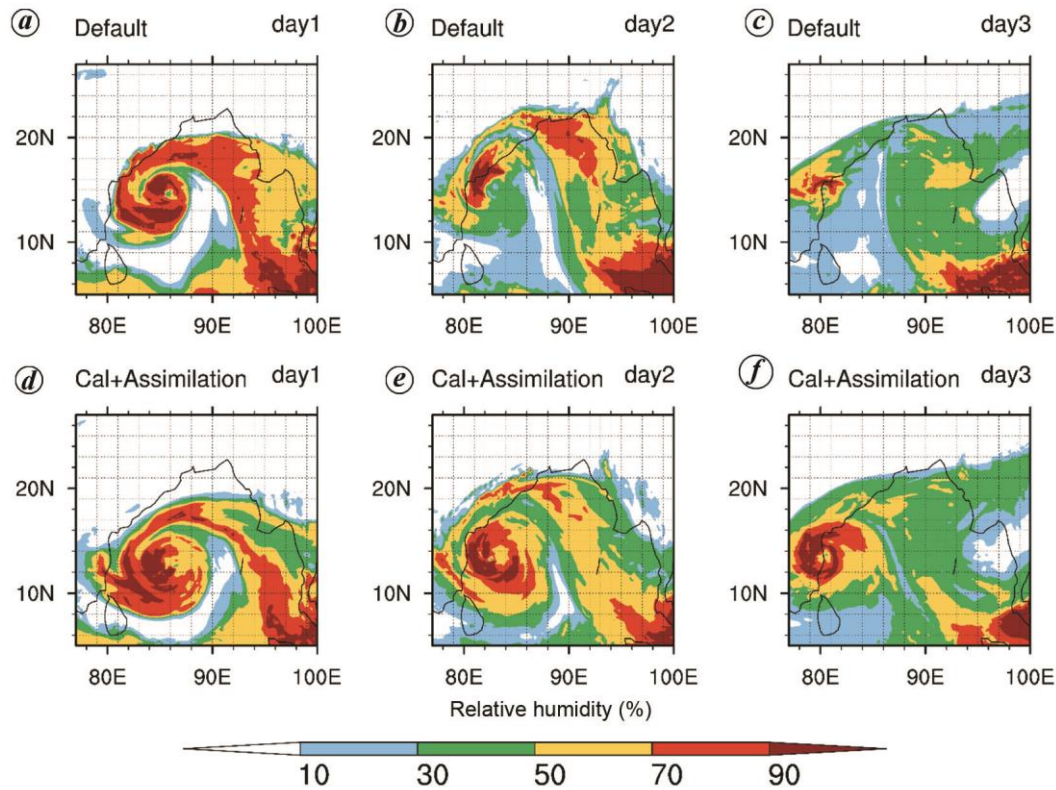
Figure 6. For the simulation of cyclone Vardah, the 500 hPa level relative humidity at the end of days 1, 2 and 3 are illustrated. Simulations using the default model without assimilation are shown in (a1–a3), while simulations using the calibrated model with assimilation are shown in (b1–b3).

experimental set-up overestimated the precipitation intensity (Supplementary Figure 3). However, the best experimental set-up simulated precipitation with a good spatial accuracy, which led to a reduction in the RMSE values compared to the default experiment (Table 4). Similar to Figure 3, the velocity field at 500 hPa for cyclone Hudhud, at the end of days 1, 2 and 3, are presented in the Supplementary Figure 4. The default and the best experimental set-up have simulated similar cyclonic circulation intensities at the end of day 1, whereas the default experiment has overestimated the cyclonic circulation intensity at the end of days 2 and 3. The same can be observed in Figure 1 m, where the default and the best experimental set-up have the same intensity at the end of day 1, and the default experiment overestimates thereafter. From these results, it is evident that the simulations with the best experimental set-up indeed improve the forecasts of precipitation and velocity.

The model forecasts of mean ascent, potential vorticity and relative humidity were spatially visualized to examine further the differences between the default and the best experimental set-up. The Supplementary Figure 5 shows that the default experiment resulted in huge spatial coverage of mean ascent with higher values at the end of all three days, compared to the best experimental set-up. This is inconsistent with the analogy that higher mean ascent will have high cyclone intensity, and this can be observed in Figure 1 m. Similar to Figure 5 for potential vorticity,

the Supplementary Figure 6 shows that the default experiment simulated intense vorticity disturbances at the end of all days, whereas the best experimental set-up simulated less intense vorticity disturbances. The Supplementary Figure 7 shows the spatial coverage of relative humidity, which also confirms the overestimation of cyclone intensity by the default experiment, whereas the best experimental set-up does it better. From these results, it is evident that the best experimental set-up not only increases or decreases the intensity for all cyclones, but closely follows the observations by improving the forecasts of precipitation, wind speed, mean ascent, potential vorticity and relative humidity.

Track and intensity predictions of cyclone Gulab

To further examine the robustness of the best experimental set-up, the cyclone track and intensity forecasts of a cyclone Gulab, simulated by the default and the best experimental set-up, are presented in the Supplementary Figure 8. The results show that the cyclone track and intensity forecasts of the default and the best experimental set-up have a close resemblance. However, the default experiment does not show landfall and underestimates the cyclone intensity. In contrast, the best experimental set-up had landfall with time delay and higher intensity than the default experiment. The RMSE values show that the best experimental set-up has a gain of 18.6% in cyclone

track forecast and 29% in cyclone intensity forecast. These results reveal that the best experimental set-up is robust compared to the default experiments from the viewpoint of several metrics.

Conclusion

This study examined the impact of multivariate BEC in the 3DVar assimilation system combined with the model calibration for the simulations of tropical cyclones over the BoB region. Seven tropical cyclones that originated during the post-monsoon period between 2012 and 2018 were selected for the experiments. The calibration model from Baki *et al.*[16] was to examine its performance with data assimilation. The multivariate BEC values of cv5, cv6, and cv7 were estimated using the 24th and 12th-hour forecasts simulated during the two-month period from 15 October to 15 December of 2016. The conventional and radiance observations were assimilated using the 3DVar system that provides the default and calibration models utilizing the multivariate BEC. The model forecasts of 10 m wind speed, precipitation, cyclone track and cyclone intensity were validated against observations. An inter-comparison of spatial structures of the prominent variables such as precipitation, 500 hPa-level velocity field, 500 hPa-level mean ascent, 500 hPa-level potential vorticity, and 500 hPa-level relative humidity was also done for cyclones Vardah and Hudhud. The main conclusions drawn from this study are summarized as follows:

- The assimilation experiments conducted with different BEC values showed variations in the RMSE values of the considered variables for all cyclones. The experiments of cv3, cv5 and cv6 showed consistent RMSE reduction for most of the cyclones; cv6 showed the best performance among all the experiments, whereas cv7 showed poor performance.
- The assimilation of conventional and radiance observations resulted similar yield to the default and calibration experiments. However, the calibration model provided an additional yield with assimilation.
- The assimilation experiments of the calibration model in combination with the cv6 BEC produced the least RMSE values compared to the remaining experiments. This was considered as the best experimental set-up.
- The results from the spatial structures indicate that the best experimental set-up simulated the cyclone intensity close to the observations by improving the predictions of wind speed, mean ascent, potential vorticity and relative humidity.

The robustness of the best experimental set-up was verified by simulating cyclone Gulab in an operational forecast. The RMSE values obtained for cyclone track and intensity confirmed the superiority of the best experimental set-up.

1. Gray, W. M., Global view of the origin of tropical disturbances and storms. *Mon. Weather Rev.*, 1968, **96**(10), 669–700.
2. Singh, O. P., Ali Khan, T. M. and Rahman, Md. S., Changes in the frequency of tropical cyclones over the north Indian Ocean. *Meteorol. Atmos. Phys.*, 2000, **75**(1–2), 11–20.
3. Deshpande, M., Singh, V. K., Ganadhi, M. K., Roxy, M. K., Emmanuel, R. and Kumar, U., Changing status of tropical cyclones over the north Indian Ocean. *Climate Dyn.*, 2021, **57**(11), 1–23.
4. Rao, D. V. B., Srinivas, D. and Satyanarayana, G. C., Trends in the genesis and landfall locations of tropical cyclones over the Bay of Bengal in the current global warming era. *J. Earth Syst. Sci.*, 2019, **128**(7), 1–10.
5. Jyoteeshkumar Reddy, P., Sriram, D., Gunthe, S. S. and Balaji, C., Impact of climate change on intense Bay of Bengal tropical cyclones of the post-monsoon season: a pseudo global warming approach. *Climate Dyn.*, 2021, **56**(9), 1–25.
6. Ooyama, K., Numerical simulation of the life cycle of tropical cyclones. *J. Atmos. Sci.*, 1969, **26**(1), 3–40.
7. Nadimpalli, R., Osuri, K. K., Pattanayak, S., Mohanty, U. C., Nageswararao, M. M. and Kiran Prasad, S., Real-time prediction of movement, intensity and storm surge of very severe cyclonic storm Hudhud over Bay of Bengal using high-resolution dynamical model. *Nat. Hazards*, 2016, **81**(3), 1771–1795.
8. Sandeep, C. P. R., Krishnamoorthy, C., and Balaji, C., Impact of cloud parameterization schemes on the simulation of cyclone Vardah using the WRF model. *Curr. Sci.*, 2018, **115**(6), 1143–1153.
9. Chandramouli, K. and Chakravarthy, B., Ingesting microwave sounder radiances for improvement in track forecast of cyclone Vardah. *J. Appl. Remote Sensing*, 2018, **12**(2), 026015.
10. Chandrasekar, R. and Balaji, C., Sensitivity of tropical cyclone Jal simulations to physics parameterizations. *J. Earth Syst. Sci.*, 2012, **121**(4), 923–946.
11. Chandrasekar, R. and Balaji, C., Impact of physics parameterization and 3DVAR data assimilation on prediction of tropical cyclones in the Bay of Bengal region. *Nat. Hazards*, 2016, **80**(1), 223–247.
12. Baki, H., Chinta, S., Balaji, C. and Srinivasan, B., A sensitivity study of WRF model microphysics and cumulus parameterization schemes for the simulation of tropical cyclones using GPM radar data. *J. Earth Syst. Sci.*, 2021, **130**(4), 1–30.
13. Di, Z. *et al.*, Assessing WRF model parameter sensitivity: a case study with 5 day summer precipitation forecasting in the Greater Beijing area. *Geophys. Res. Lett.*, 2015, **42**(2), 579–587.
14. Kalnay, E., *Atmospheric Modeling, Data Assimilation and Predictability*, Cambridge University Press, Cambridge, 2003.
15. Yang, B., Qian, Y., Lin, G., Leung, R. and Zhang, Y., Some issues in uncertainty quantification and parameter tuning: a case study of convective parameterization scheme in the WRF regional climate model. *Atmos. Chem. Phys.*, 2012, **12**(5), 2409–2427.
16. Baki, H., Chinta, S., Balaji, C. and Srinivasan, B., WRF model parameter calibration to improve the prediction of tropical cyclones over the Bay of Bengal using machine learning-based multiobjective optimization. arXiv preprint arXiv:2110.05817, 2021.
17. Singh, R., Kishtawal, C. M., Pal, P. K. and Joshi, P. C., Assimilation of the multisatellite data into the WRF model for track and intensity simulation of the Indian Ocean tropical cyclones. *Meteorol. Atmos. Phys.*, 2011, **111**(3–4), 103–119.
18. Ha, J. H. and Lee, D. K., Effect of length scale tuning of background error in WRF-3DVAR system on assimilation of high-resolution surface data for heavy rainfall simulation. *Adv. Atmos. Sci.*, 2012, **29**(6), 1142–1158.
19. Osuri, K. K., Mohanty, U. C., Routray, A. and Mohapatra, M., The impact of satellite-derived wind data assimilation on track, intensity, and structure of tropical cyclones over the North Indian Ocean. *Int. J. Remote Sensing*, 2012, **33**(5), 1627–1652.

20. Yesubabu, V., Srinivas, C. V., Hariprasad, K. B. R. R. and Baskaran, R., A study on the impact of observation assimilation on the numerical simulation of tropical cyclones JAL and THANE using 3DVAR. *Pure Appl. Geophys.*, 2014, **171**(8), 2023–2042.

21. Dhanya, M., Gopalakrishnan, D., Chandrasekar, A., Singh, S. K. and Prasad, V. S., The impact of assimilating Megha Tropiques SAPHIR radiances in the simulation of tropical cyclones over the Bay of Bengal using the WRF model. *Int. J. Remote Sensing*, 2016, **37**(13), 3086–3103.

22. Gopalakrishnan, D. and Chandrasekar, A., On the improved predictive skill of WRF model with regional 4DVar Initialization: a study with north Indian Ocean tropical cyclones. *IEEE Trans. Geosci. Remote Sensing*, 2018, **56**(6), 3350–3357.

23. Gopalakrishnan, D. and Chandrasekar, A., Improved 4DVar simulation of Indian Ocean tropical cyclones using a regional model. *IEEE Trans. Geosci. Remote Sensing*, 2018, **56**(9), 5107–5114.

24. Kutty, G., Gogoi, R., Rakesh, V. and Pateria, M., Comparison of the performance of hybrid etkf-3dvar and 3dvar data assimilation scheme on the forecast of tropical cyclones formed over the Bay of Bengal. *J. Earth Syst. Sci.*, 2020, **129**(1), 1–14.

25. Bannister, R. N., A review of forecast error covariance statistics in atmospheric variational data assimilation. i: Characteristics and measurements of forecast error covariances. *Q. J. R. Meteorol. Soc. J. Atmosph. Sci., Appl. Meteorol. Phys. Oceanogr.*, 2008, **134**(637), 1951–1970.

26. Rakesh, V. and Goswami, P., Impact of background error statistics on forecasting of tropical cyclones over the north Indian Ocean. *J. Geophys. Res. Atmosp.*, 2011, **116**(20), 1–21.

27. Dhanya, M. and Chandrasekar, A., Multivariate background error covariances in the assimilation of SAPHIR radiances in the simulation of three tropical cyclones over the Bay of Bengal using the WRF model. *Int. J. Remote Sensing*, 2018, **39**(1), 191–209.

28. Thiruvengadam, P., Indu, J. and Ghosh, S., Improving convective precipitation forecasts using ensemble-based background error covariance in 3DVAR radar assimilation system. *Earth Space Sci.*, 2020, **7**(4), 1–11.

29. Skamarock, W. C., Klemp, J. B., Dudhia, J., Gill, D. O., Barker, D., Duda, M. G. and Powers, J. G., A description of the Advanced Research WRF version 3 (No. NCAR/TN-475+STR). University Corporation for Atmospheric Research; doi:10.5065/D68S4MVH.

30. Kain, J. S., The Kain–Fritsch convective parameterization: an update. *J. Appl. Meteorol.*, 2004, **43**(1), 170–181.

31. Beljaars, A. C. M., The parametrization of surface fluxes in large-scale models under free convection. *Q. J. R. Meteorol. Soc.*, 1995, **121**(522), 255–270.

32. Hong, S.-Y. and Lim, J.-O. J., The WRF single-moment 6-class microphysics scheme (WSM6). *Asia-Pac. J. Atmos. Sci.*, 2006, **42**(2), 129–151.

33. Mlawer, E. J., Taubman, S. J., Brown, P. D., Iacono, M. J. and Clough, S. A., Radiative transfer for inhomogeneous atmospheres: RRTM, a validated correlated-k model for the longwave. *J. Geophys. Res.: Atmos.*, 1997, **102**(D14), 16663–16682.

34. Tewari, M. *et al.*, Implementation and verification of the unified NOAH land surface model in the WRF model (formerly paper number 17.5). In Proceedings of the 20th Conference on Weather Analysis and Forecasting/16th Conference on Numerical Weather Prediction, Seattle, WA, USA, 2004, pp. 11–15.

35. Dudhia, J., Numerical study of convection observed during the winter monsoon experiment using a mesoscale two-dimensional model. *J. Atmos. Sci.*, 1989, **46**(20), 3077–3107.

36. Hong, S.-Y., Noh, Y. and Dudhia, J., A new vertical diffusion package with an explicit treatment of entrainment processes. *Month. Weather Rev.*, 2006, **134**(9), 2318–2341.

37. Thiruvengadam, P., Indu, J. and Ghosh, S., Improving convective precipitation forecasts using ensemble-based background error covariance in 3DVar radar assimilation system. *Earth Space Sci.*, 2020, **7**(4), e2019EA000667.

38. Parrish, D. F. and Derber, J. C., The National Meteorological Center's spectral statistical interpolation analysis system. *Month. Weather Rev.*, 1992, **120**(8), 1747–1763.

39. National Centers for Environmental Prediction, National Weather Service, NOAA, US Department of Commerce. NCEP ADP global upper air and surface weather observations (prepbufr format), NCEP, USA, 2008.

40. National Centers for Environmental Prediction, National Weather Service, NOAA, US Department of Commerce, NCEP GDAS satellite data 2004-continuing. NCEP, USA, 2009.

41. Huffman, G. and Savtchenko, A. K., GPM IMERG final precipitation L3 half hourly 0.1 degree × 0.1 degree V06, 2019 (accessed on 23 September 2020).

42. Indira Rani, S. *et al.*, Imdaa: high-resolution satellite-era reanalysis for the Indian monsoon region. *J. Climate*, 2021, **34**(12), 5109–5133.

43. Yesubabu, V., Srinivas, C. V., Hariprasad, K. B. R. R. and Baskaran, R., A study on the impact of observation assimilation on the numerical simulation of tropical cyclones Jal and Thane using 3dVar. *Pure Appl. Geophys.*, 2014, **171**(8), 2023–2042.

44. Dhanya, M. and Chandrasekar, A., Multivariate background error covariances in the assimilation of Saphir radiances in the simulation of three tropical cyclones over the Bay of Bengal using the WRF model. *Int. J. Remote Sensing*, 2018, **39**(1), 191–209.

45. Zhao, M. and Held, I. M., TC-permitting GCM simulations of hurricane frequency response to sea surface temperature anomalies projected for the late-twenty-first century. *J. Climate*, 2012, **25**(8), 2995–3009.

46. Bell, R., Strachan, J., Vidale, P.-L., Hodges, K. and Roberts, M., Response of tropical cyclones to idealized climate change experiments in a global high-resolution coupled general circulation model. *J. Climate*, 2013, **26**(20), 7966–7980.

47. Jackson, L. S. *et al.*, The effect of explicit convection on couplings between rainfall, humidity, and ascent over Africa under climate change. *J. Climate*, 2020, **33**(19), 8315–8337.

48. Ma, L.-M. and Tan, Z.-M., Improving the behavior of the cumulus parameterization for tropical cyclone prediction: convection trigger. *Atmos. Res.*, 2009, **92**(2), 190–211.

49. Emanuel, K., DesAutels, C., Holloway, C. and Korty, R., Environmental control of tropical cyclone intensity. *J. Atmos. Sci.*, 2004, **61**(7), 843–858.

50. Hendricks, E. A., Peng, M. S., Fu, B. and Li, T., Quantifying environmental control on tropical cyclone intensity change. *Month. Weather Rev.*, 2010, **138**(8), 3243–3271.

51. Kaplan, J., DeMaria, M. and Knaff, J. A., A revised tropical cyclone rapid intensification index for the Atlantic and eastern north Pacific basins. *Weather Forecast.*, 2010, **25**(1), 220–241.